Metabolic Engineering Communications 16 (2023) e00220

Contents lists available at ScienceDirect

Metabolic Engineering Communications

journal homepage: www.elsevier.com/locate/mec

Metabolic engineering of low-pH-tolerant non-model yeast, *Issatchenkia orientalis*, for production of citramalate

Zong-Yen Wu [a,1], Wan Sun [b,l,1], Yihui Shen [c,d], Jimmy Pratas [c,d], Patrick F. Suthers [e,f], Ping-Hung Hsieh [g], Sudharsan Dwaraknath [g], Joshua D. Rabinowitz [c,d], Costas D. Maranas [e,f], Zengyi Shao [b,h,i,j,k,l,**], Yasuo Yoshikuni [a,m,n,o,*]

[a] *Environmental Genomics and Systems Biology Division, Lawrence Berkeley National Laboratory, Berkeley, CA, 94720, USA*
[b] *Interdepartmental Microbiology Program, Iowa State University, Ames, IA, 50011-1027, USA*
[c] *Department of Chemistry, Princeton University, Princeton, NJ, 08544, USA*
[d] *Lewis Sigler Institute for Integrative Genomics, Princeton University, Princeton, NJ, 08540, USA*
[e] *Department of Chemical Engineering, The Pennsylvania State University, University Park, PA, 16802, USA*
[f] *Center for Advanced Bioenergy and Bioproducts Innovation, The Pennsylvania State University, University Park, PA, 16802, USA*
[g] *US Department of Energy Joint Genome Institute, Lawrence Berkeley National Laboratory, Berkeley, CA, 94720, USA*
[h] *Department of Chemical and Biological Engineering, Iowa State University, Ames, IA, 50011, USA*
[i] *NSF Engineering Research Center for Biorenewable Chemicals, Iowa State University, Ames, IA, 50011, USA*
[j] *Bioeconomy Institute, Iowa State University, Ames, IA, 50011, USA*
[k] *The Ames Laboratory, Ames, IA, 50011, USA*
[l] *DOE Center for Advanced Bioenergy and Bioproducts Innovation, University of Illinois at Urbana-Champaign, Urbana, IL, 61801, USA*
[m] *Biological Systems and Engineering Division, Lawrence Berkeley National Laboratory, Berkeley, CA, 94720, USA*
[n] *Center for Advanced Bioenergy and Bioproducts Innovation, Lawrence Berkeley National Laboratory, Berkeley, CA, 94720, USA*
[o] *Global Center for Food, Land, and Water Resources, Hokkaido University, Hokkaido, 060-8589, Japan*

ARTICLE INFO

Handling Editor: Mattheos Koffas

Keywords:
Poly(methyl methacrylate) (PMMA)
Issatchenkia orientalis
Citramalate
Acid tolerance
Transposon

ABSTRACT

Methyl methacrylate (MMA) is an important petrochemical with many applications. However, its manufacture has a large environmental footprint. Combined biological and chemical synthesis (semisynthesis) may be a promising alternative to reduce both cost and environmental impact, but strains that can produce the MMA precursor (citramalate) at low pH are required. A non-conventional yeast, *Issatchenkia orientalis*, may prove ideal, as it can survive extremely low pH. Here, we demonstrate the engineering of *I. orientalis* for citramalate production. Using sequence similarity network analysis and subsequent DNA synthesis, we selected a more active citramalate synthase gene (*cimA*) variant for expression in *I. orientalis*. We then adapted a piggyBac transposon system for *I. orientalis* that allowed us to simultaneously explore the effects of different *cimA* gene copy numbers and integration locations. A batch fermentation showed the genome-integrated-*cimA* strains produced 2.0 g/L citramalate in 48 h and a yield of up to 7% mol citramalate/mol consumed glucose. These results demonstrate the potential of *I. orientalis* as a chassis for citramalate production.

1. Introduction

Methyl methacrylate (MMA) is a building block for poly MMA (PMMA), which is a transparent material known as acrylic glass or plexiglass with the trade names Acrylite® and Plexiglas® (Mahboub et al., 2018). PMMA is an economical alternative to polycarbonate (PC) and has diverse industrial applications (including paints, coatings, electronics, and modifier for polyvinyl chloride [PVC]) (Dixit et al., 2009; Lebeau et al., 2020; Mahboub et al., 2018). PMMA is also commonly used in making prosthetic dental applications, including dentures, denture bases, and artificial teeth (implants) (Frazer et al., 2005; Zafar, 2020). Because of MMA's versatility, its global market

* Corresponding author. Environmental Genomics and Systems Biology Division, Lawrence Berkeley National Laboratory, Berkeley, CA, 94720, USA.
** Corresponding author. Interdepartmental Microbiology Program, Iowa State University, Ames, IA, 50011-1027, USA.
E-mail addresses: zyshao@iastate.edu (Z. Shao), yyoshikuni@lbl.gov (Y. Yoshikuni).
[1] These authors contributed equally.

https://doi.org/10.1016/j.mec.2023.e00220
Received 29 November 2022; Received in revised form 8 February 2023; Accepted 14 February 2023
Available online 16 February 2023

demand is expected to grow to USD 8.16 billion by 2025, with a compound annual growth rate of 8.4% (Grand View Research, 2019).

MMA is currently produced from petroleum using chemical processes. The dominant commercial process for MMA is the acetone cyanohydrin (ACH) route. The use of toxic hydrogen cyanide and concentrated acid is a primary concern for the ACH route, as are the negative impacts of co-product waste (ammonium bisulfate) generation and disposal. (Lebeau et al., 2020; Mahboub et al., 2018; Nagai and Ui, 2004). Although the industry has improved the process significantly, even the safer and more-sustainable alternatives recently developed are still energy-intensive, and therefore contribute excessively to greenhouse gas emission. For example, the LiMA process, milder than others, emits 2.6 t-CO_2/t-MMA (Mahboub et al., 2018).

Producing MMA from renewable resources may be a more attractive alternative. Semisynthesis (a combination of biological and chemical processes) may be the best strategy for MMA production, as MMA is toxic to cells because of its lipophilicity and reactivity with cellular components, and no enzyme is currently known to directly catalyze the formation of MMA (Curson et al., 2014; Webb et al., 2018). Diverse metabolites have been proposed as precursors for MMA production (Lebeau et al., 2020). Among them, the most promising approach may be to use di- and tricarboxylic acid metabolites as precursors. In particular, we selected citramalate, a dicarboxylic acid, as a target for semisynthesis because it can easily be converted to methacrylic acid (MA), a precursor for MMA, via base-catalyzed decarboxylation and dehydration in hot pressurized water (Johnson et al., 2015; Wu and Eiteman, 2016). MA is then converted into MMA through esterification in the presence of methanol and an acid catalyst (Lebeau et al., 2020).

Citramalate is a common metabolite found in diverse organisms as an intermediate of the isoleucine biosynthesis pathway (Risso et al., 2008; Sugimoto et al., 2021). The key enzyme for citramalate synthesis is citramalate synthase (CimA, EC 2.3.1.182), which catalyzes condensation of the central metabolites pyruvate and acetyl-CoA to generate citramalate (Howell et al., 1999). An *E. coli* strain has been engineered to produce citramalate. This strain carried an exogenous citramalate synthase gene (*cimA*) with the genes for lactate dehydrogenase (*ldh*) and pyruvate formate lyase (*pfl*) deleted. The low toxicity of citramalate compared to many other organic acids helped increase its production significantly. Fed-batch fermentation using this *E. coli* strain achieved a titer of 82 g/L, a productivity of 1.85 g L^{-1} hr^{-1}, and a conversion yield of 0.48 wt% (Webb et al., 2018).

One major bottleneck for this process, however, is that a neutralization step is required. At a large scale of production, a cheap alkali source, lime ($CaCO_3$), is generally used for the neutralization, which results in high CO_2 emission. Additionally, the media must be reacidified with H_2SO_4 to convert the salt form to the undissociated form of citramalate, resulting in formation of a large amount of gypsum ($CaSO_4$) as a byproduct that needs to be properly disposed. The technoeconomic assessment and life cycle assessment for organic acid production suggest that neutralization and acidification steps increase both process cost and environmental footprint by 30% (Bhagwat et al., 2021). Low-pH fermentation using acid-tolerant microbes are therefore a better process for citramalate production.

Acknowledging the benefits of low-pH fermentation, the US Department of Energy's Center for Bioenergy and Bioproduct Innovations (CABBI) selected *Issatchenkia orientalis* as its flagship strain for organic acid production because of its ability to tolerate extremely low pH. *I. orientalis* has already been engineered to produce some organic acids, including D-xylonic acid (Toivari et al., 2013), succinic acid (Xiao et al., 2014), D-lactic acid (Park et al., 2018), itaconic acid (Sun et al., 2020), and 3-hydroxypropionic acid (Bindel, 2016). With recent advances in genetic and genomic engineering tools (e.g., plasmid, promoters, terminators, and CRISPR-Cas9 system) (Cao et al., 2020; Tran et al., 2019) and a genome-scale metabolic model, *iIsor*850 (Suthers et al., 2020), *I. orientalis* is becoming a more amenable strain for metabolic engineering.

In this study, we attempted to engineer *I. orientalis* for production of citramalate. We first screened *cimA* genes and identified a more active variant in *I. orientalis*. To stably integrate this *cimA* gene variant into *I. orientalis*'s genome, we employed a hyperactive piggyBac transposase system (Li et al., 2013; Wagner et al., 2018; Yusa et al., 2011) and generated a *cimA* integration library. This system allows us to explore the effect of both various *cimA* integration locations and different numbers of *cimA* integration copy on citramalate production. Subsequent screening of this library identified a citramalate producer that was drastically better than its plasmid-based counterpart.

2. Materials and methods

2.1. Strains, media, and chemicals

The strains used in this study are listed in Supplementary Table S1. Dr. Hulmin Zhao (University of Illinois Urbana-Champaign) kindly provided *I. orientalis* SD108, *I. orientalis* SD108 *ΔURA3*, and *I. orientalis* SD108 *ΔURA3 ΔLEU2*, which were used as hosts for citramalate production. *S. cerevisiae* YSG50 (*MATα, ADE2-1, ADE3Δ22, URA3-1, HIS3-11,15, TRP1-1, LEU2-3,112, and CAN1-100*) was the host for plasmid assembly using the DNA assembler (Shao et al., 2012; Shao and Zhao, 2014). *E. coli* strain BW25141 was used for plasmid propagation. Yeast extract-peptone-dextrose (YPD) medium containing 1% yeast extract, 2% peptone, and 2% dextrose was used to grow yeast strains. Yeast nitrogen base with amino acids (YNB) containing 2% glucose was used for pH and citramalate tolerance analysis. Synthetic complete dropout medium without uracil (SC-URA) or leucine (SC-LEU) containing 0.5% ammonium sulfate, 0.16% yeast nitrogen base without amino acid or ammonium sulfate, CSM-URA/LEU (added according to manufacturer's instruction), 0.043% adenine hemisulfate, and 2% dextrose were used to select the yeast transformants containing the auxotrophic selection plasmid. 0.1 mg/mL 5-fluoroorotic acid (5-FOA, GoldBio, St Louis, MO) was added to the SC-LEU plate for URA3 counterselection unless otherwise stated. Luria−Bertani (LB) broth supplemented with 100 μg/mL ampicillin was used to grow *E. coli* strains. The Wizard Genomic DNA Purification Kit was purchased from Promega (Madison, WI). FastDigest restriction enzymes were purchased from Thermo Fisher Scientific (Waltham, MA). Q5 DNA polymerase was purchased from New England Biolabs (Ipswich, MA). The QIAprep Spin Plasmid Mini-prep Kit and RNeasy Mini Kit were purchased from Qiagen (Valencia, CA). Zymoprep Yeast Plasmid Miniprep II Kit was purchased from Zymo Research (Irvine, CA). Oligonucleotides and gBlocks were synthesized by Integrated DNA Technologies (Coralville, IA).

2.2. pH and citramalate tolerance analysis

To test the pH tolerance of *I. orientalis* SD108, we first streaked the glycerol stock of this strain on a YPD plate and grew it overnight at 30 °C. A single colony was picked up from the plate and inoculated in 2 mL YNB broth containing 2% glucose with an initial pH of 5.3, then grown overnight at 30 °C with constant shaking at 250 rpm on a platform shaker. The 2 mL seed culture was pelleted and diluted in the same fresh YNB broth (containing 2% glucose at pH 5.3) with an OD_{600} of 1.5, and then grown at 30 °C with constant shaking at 250 rpm on a platform shaker for 2 h. Then the culture was pelleted and diluted to an OD_{600} of 0.1 in the same YNB/glucose broth at various pH values (1.5, 2.0, 2.5, 3.0, 3.5, and 5.5), adjusted by HCl. 200 μL cultures from each condition were added to the wells, and OD_{600} was measured every 30 min for 60.5 h at 30 °C with constant shaking in a plate reader. The same protocol was applied to test the tolerance of citramalate at 40 g/L and 80 g/L at pH 3.0 with various concentrations of citramalate (Sigma-Aldrich SKU-27455 Potassium citramalate monohydrate). 200 μL cultures from each condition were added to the wells, and OD_{600} was measured every 30 min for 96.5 h at 30 °C with constant shaking in a plate reader.

2.3. CimA sequence similarity network construction and target gene selection

The CimA sequence similarity network (SSN) was constructed using the Enzyme Function Initiative-Enzyme Similarity Tool (EFI-EST) (Gerlt et al., 2015). A well-studied CimA from *Methanocaldococcus jannaschii* (UniProt ID Q58787) was used as the query for SSN construction. Cytoscape was used to visualize the SSN (Shannon et al., 2003). An overview of the CimA SSN used in this study is provided in Supplementary Table S2. We first selected genes that had been reported in the literature and subsequently included genes with eukaryotic origins. We also chose the sequences randomly from different clusters in which the UniProt annotation score was greater than 3. Among the 10 selected genes, we optimized the codon usage using JGI Build-Optimization Software Tools (BOOST) (Oberortner et al., 2017) with different strategies to minimize the chance that the codon optimization would accidently design sequences resulting in poor expression. We then purchased the synthetic gene fragments from Twist Bioscience. We synthesized these genes with "balanced" and "mostly used" strategies (Supplementary Table S3) in which each of the DNA sequences statistically resembles the *I. orientalis* codon usage table (Nakamura, 2007). The least-used codons were eliminated (Supplementary Table S4).

2.4. Plasmid construction

The plasmids used in this study are listed in Supplementary Table S1. The *cimA* expression vector pZF_TDH3p with URA3 selection marker was used for identifying an *I. orientalis*-compatible *cimA* gene. The TDH3 promoter drives the synthetic *cimA* gene; ENO2 was used as the terminator in this plasmid. We introduced an EcoR1 cutting site between the TDH3 promoter and the ENO2 terminator to generate pZF_EcoR1_TDH3, which allowed cloning of the synthetic *cimA* gene into pZF_EcoR1_TDH3p (Supplementary Fig. S1). To construct the plasmid for *cimA* genome integration, we amplified the centromere-like sequence, autonomously replicating sequence (ARS), and URA3 cassette from pScARS/CEN-L and assembled them as the backbone (Cao et al., 2020). Both pZF_TDH3p and pSsARS/CEN-L vectors were provided by Dr. Hulmin Zhao's group from the University of Illinois at Urbana-Champaign. We codon-optimized and synthesized the hyperactive piggyBac transposase hPB7 variant (I30V, G165S, S103P, M282V, S509G/N570S, and N538K) (Yusa et al., 2011), and then cloned it under the control of the INO1 promoter and the SED1 terminator. We enclosed the *cimA* cassette flanked by a green fluorescence protein (GFP) cassette and a LEU cassette in the two piggyBac inverted terminal repeats (ITRs) sequence (5′ITR-GFP-CimA-LEU-3′ITR) and assembled them together with an *E. coli* helper fragment amplified from pRS416. The assembly was performed in *S. cerevisiae* YSG50 via DNA assembler (Shao et al., 2012; Shao and Zhao, 2014). The plasmid was confirmed by restriction digestion and sequencing and named pWS-URA-hPB7-GFP-CimA-LEU (Supplementary Fig. S2).

2.5. Purification and in vitro characterization of CimA variants

I. orientalis cells expressing citramalate synthase variants (attached with a C-terminal His-tag) were grown in SC-URA medium. A 5 mL overnight culture was used to inoculate 100 mL of media in 500 mL flasks to a starting OD_{600} of 0.1. Cultures were grown at 30 °C at 200 rpm for 20 h. The suspensions were pelleted, washed, and lysed using a CelLytic Y lysis reagent (Sigma-Aldrich) that included 10 mM DTT, according to the manufacturer's instructions. The lysate was passed through a desalting column and purified by Ni-NTA spin column chromatography (Qiagen). Enzyme concentration was measured by Bradford Assay using the Pierce Coomassie Protein Assay Kit (Thermo Scientific). The specific activity of citramalate biosynthesis *in vitro* was measured by incubating 0.1 μM enzyme, 1 mM acetyl-CoA, and 20 mM sodium pyruvate in 100 mM TES buffer at pH 7.5 at 30 °C for 50 min following a procedure reported earlier (Howell et al., 1999).

2.6. Strain construction

The strains used in this study are listed in Supplementary Table S1. To identify the compatibility of the synthetic *cimA* gene in *I. orientalis*, we transformed the *cimA* expression plasmids into *I. orientalis* SD108 *ΔURA3* using the Frozen-EZ Yeast Transformation II Kit (Zymo Research) and following the manufacturer's instructions. After the transformation, the cells were washed with sterile distilled water once and resuspended in 500 μL SC-URA broth, then cultivated at 30 °C for 2 h 150 μL of cell culture was spread across the surface of the SC-URA agar plate, and then incubated for 48 h at 30 °C. Colonies were randomly picked for further PCR confirmation. To construct genome-integrated-*cimA* strains using piggyBac-mediated transposition, about 1 μg of pWS-URA-hPB7-GFP-CimA-LEU was transformed into *I. orientalis* SD108 *ΔURA3 ΔLEU2* by electroporation at 2.0 kV and selected on an SC-LEU plate. To enable efficient transposase expression and DNA transposition, the colonies that appeared on the plate were washed into approximately 10 mL SC-LEU broth and grown at 30 °C at 250 rpm for 3 days according to a previous transposition study in *Yarrowia lipolytica* (Wagner et al., 2018). The cell culture was then diluted and spread on both SC-LEU and SC-LEU+5FOA plates. Colonies that grew on SC-LEU+5FOA plates were collected as the genome-integrated-*cimA* strain library.

2.7. Flow cytometry

50 single colonies from the genome-integrated-*cimA* strain library were picked from the SC-LEU + FOA plate and grown in 2 mL SC-LEU medium for 24–36 h. Then 10 μL of the cell culture was diluted in 10 mM phosphate-buffered saline (pH 7.4) and analyzed by flow cytometry at 488 nm with a FACSCanto flow cytometer (BD Biosciences, San Jose, CA) for GFP. BD FACSCanto clinical software was used to evaluate the flow cytometry data.

2.8. Plasmid removal

To make sure there was no plasmid left in the genome-integrated-*cimA* strain, four top citramalate-producing strains were grown in 2 mL SC-LEU broth supplemented with 2 g/L 5FOA for 2 days, then spread on SC-LEU+5FOA plates. After colonies were seen on plates, single colonies were picked and duplicated on both SC-URA and SC-LEU+5FOA plates. Colonies that could only grow on SC-LEU + FOA plates were our final genome-integrated-*cimA* strains. To ensure that the strains only have stably expressed genomic *cimA*, 5-FOA counterselection was performed to cure the piggyBac-expressing plasmid. It is worth pointing out that our final four top producers SB814, SB815, SB816, and SB817 were generated through 2-step counterselection. During the construction of the *cimA*-integrated *I. orientalis* strain, the transformants on SC-LEU plates were re-streaked on SC-LEU+5FOA plates. Presumably, the original plasmids or the re-ligated plasmids post-transposition were cured. However, the re-streaked cells were still able to grow in the SC-URA broth. A second-step counterselection was performed by growing the colonies from SC-LEU+5FOA plates in liquid SC-LEU+5FOA medium for 1–2 days and spreading onto SC-LEU+5FOA plates. The plasmid cure was verified by picking the colonies that grew on a SC-LEU+5FOA plate but not on a SC-URA plate.

2.9. Citramalate production

To compare transformants with various *cimA* sequences, cells were harvested from a fresh agar culture plate, and then resuspended in 50 mL SC-URA to let the starting OD_{600} reach 2. After growth at 30 °C at 200 rpm for 24 h, the supernatants were centrifuged (800 g, 5 min) and filtered (0.45 μm), then analyzed for citramalate concentration using

high-performance liquid chromatography (HPLC) analysis. To select top citramalate producers from the genome-integrated-*cimA* strain library, strains that were confirmed to have a genome-integrated version of GFP were inoculated in 10 mL SC-LEU broth and cultured for about 1 day. Cell pellets were collected by centrifugation, washed twice with water, transferred into 10 mL of SC-LEU with 50 g/L glucose liquid medium with an initial OD_{600} of 1, and cultivated at 30 °C with 250 rpm orbital shaking in 55 mL glass tubes. Samples (1 mL cell culture) were collected after 5-day growth for citramalate analysis. After removal of URA plasmid from top citramalate producers, the new genome-integrated-*cimA* strains were cultivated under different media (SC+50 g/L glucose and YPD+50 g/L glucose) and compared with the plasmid version strain SD108 *ura3Δ* pCimA03 for quantifying metabolite production, using the wild-type SD108 used as a control strain. Seed cultures were grown in 10 mL YPD liquid medium and cultured for about 1.5 day. The fermentation condition was the same as for the abovementioned method except that samples (0.5 mL cell culture) were collected at 24 h, 48 h, and 72 h, and ODs were also measured. The experiments were conducted with three biological replicates.

2.10. HPLC and LC-MS analysis

To identify *I. orientalis* strains with active *cimA* genes, the spent media samples (500 μL) were analyzed using a Shimadzu system with refractive index detectors, using a Rezex ROA Organic Acid H^+ column at 55 °C with 5 mM H_2SO_4 (0.5 mL min^{-1}) as the mobile phase. Citramalate was identified by comparing the retention times with commercial standards (Sigma), and concentrations were determined from calibration curves. For quantification of citramalate production after fermentation, spent media was analyzed by an Agilent 6495C liquid chromatography mass spectrometer (LC-MS), equipped with an electron spray ionization source coupled to a triple quadrupole mass analyzer. The spent media was diluted 50–300 fold into 40:40:20 methanol: acetonitrile:water. Chemical separation was based on hydrophilic interaction liquid chromatography (HILIC) with an XBridge BEH Amide column (2.1 mm × 150 mm, 2.5 μm particle size, 130 Å pore size; Waters), with a solvent gradient as follows: 10% A at 0 min, 25% A at 3 min, 30% A at 8 min, 50% A at 10 min, 75% A at 13 min, 100% A at 16 min, 10% A at 21 min (solvent A is 20 mM ammonia and 20 mM ammonium acetate in water with 5% acetonitrile, pH 9; solvent B is 100% acetonitrile), and a flow rate of 150 μL/min. The mass spectrometer operated in a multiple reaction monitoring mode with negative ionization. The particular reactions (precursor ion - > product ion) and collision energies were: glucose, 179 -> 89, 15 V; citramalate, 147 -> 85, 15 V; glycerol, 91 -> 59, 15 V; pyruvate, 87 -> 43, 12 V. For quantitation, a mixture of standards was prepared in a series of concentrations, similarly analyzed, and then used to obtain external calibration curves. Data were converted to mzXML format by msconvert (proteowizard) (Chambers et al., 2012) and analyzed by El-Maven software (Elucidata).

3. Results

3.1. pH and citramalate tolerance of I. orientalis SD108

We initially tested *I. orientalis*'s ability to tolerate low pH and high citramalate concentration to evaluate the potential of using *I. orientalis* as a host for citramalate production using a low-pH fermentation process. As shown in Fig. 1A, growth curves for *I. orientalis* SD108 were similar over a wide range, from a pH of 2.0 to a pH of 5.5. This result is consistent with results from a previous study (Xiao et al., 2014). Measuring cell density at 10 h of cultivation, Xiao et al. concluded that optimal growth of *I. orientalis* SD108 occurred at a pH range of 3 and 6. To our surprise, we analyzed growth curves and found that *I. orientalis* SD108 can grow at a pH of as low as 1.5, although at that pH the growth rate was slower than it was under other pH values (Fig. 1A). At a pH of 1.5, *I. orientalis* SD108 took 40 h to reach an OD_{600} of 0.9, which was approximately 4 times longer than the time it took to reach the same density at pHs of 2.5, 3.0, 3.5, and 5.5. Additionally, we evaluated the ability of *I. orientalis* SD108 to tolerate citramalate at two different concentrations (40 g/L and 80 g/L). We set this culture pH at 3.0 because the pKa of citramalate is around 3.35, and we expected that the culture pH would be maintained around the pKa of citramalate. We found that *I. orientalis* SD108 could tolerate 80 g/L of citramalate at pH 3.0 and maintain a growth rate of about 50% of the control's (Fig. 1B). These properties of *I. orientalis* SD108 make it an ideal candidate as a host platform for production of citramalate through a low-pH fermentation process.

3.2. Identification of cimA for citramalate production in I. orientalis

To produce citramalate efficiently, we first sought a *cimA* variant more compatible with expression in *I. orientalis* and thereby better for citramalate production (Fig. 2A). We built the SSN and selected ten *cimA* variants to maximize the sampling space across the SSN (Fig. 2B). We subsequently synthesized these genes, cloned them into a plasmid, expressed them in *I. orientalis*, and measured citramalate production. Five out of the ten genes showed citramalate synthase activity. The two strains carrying *cimA* gene #03 (*Methanocaldococcus jannasch*) (one synthesized using a "balanced" codon optimization strategy, the other using a "mostly used" strategy) averaged the highest productivity in citramalate production (0.64 g/L and 0.74 g/L, respectively) (Fig. 2C). The two strains carrying *cimA* gene #08 (*Streptomyces coelicolor*) averaged the second highest productivity in citramalate production (0.63 g/L and 0.64 g/L, respectively) (Fig. 2C). We then evaluated these two

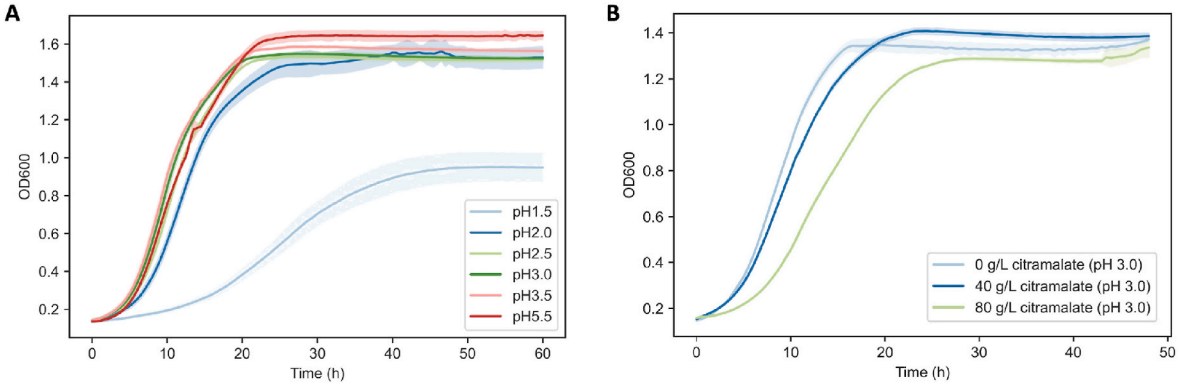

Fig. 1. Tolerance of *I. orientalis* SD108 to various pH values and citramalate concentrations. (A) Growth curve measured in YNB broth at various pH values (1.5, 2.0, 2.5, 3.0, 3.5, and 5.5) at 30 °C. (B) Growth curve measured in YNB broth with various citramalate concentrations at pH 3.0. We collected the data in biological triplicate. The shaded areas indicate the standard deviation of the triplicate measurements.

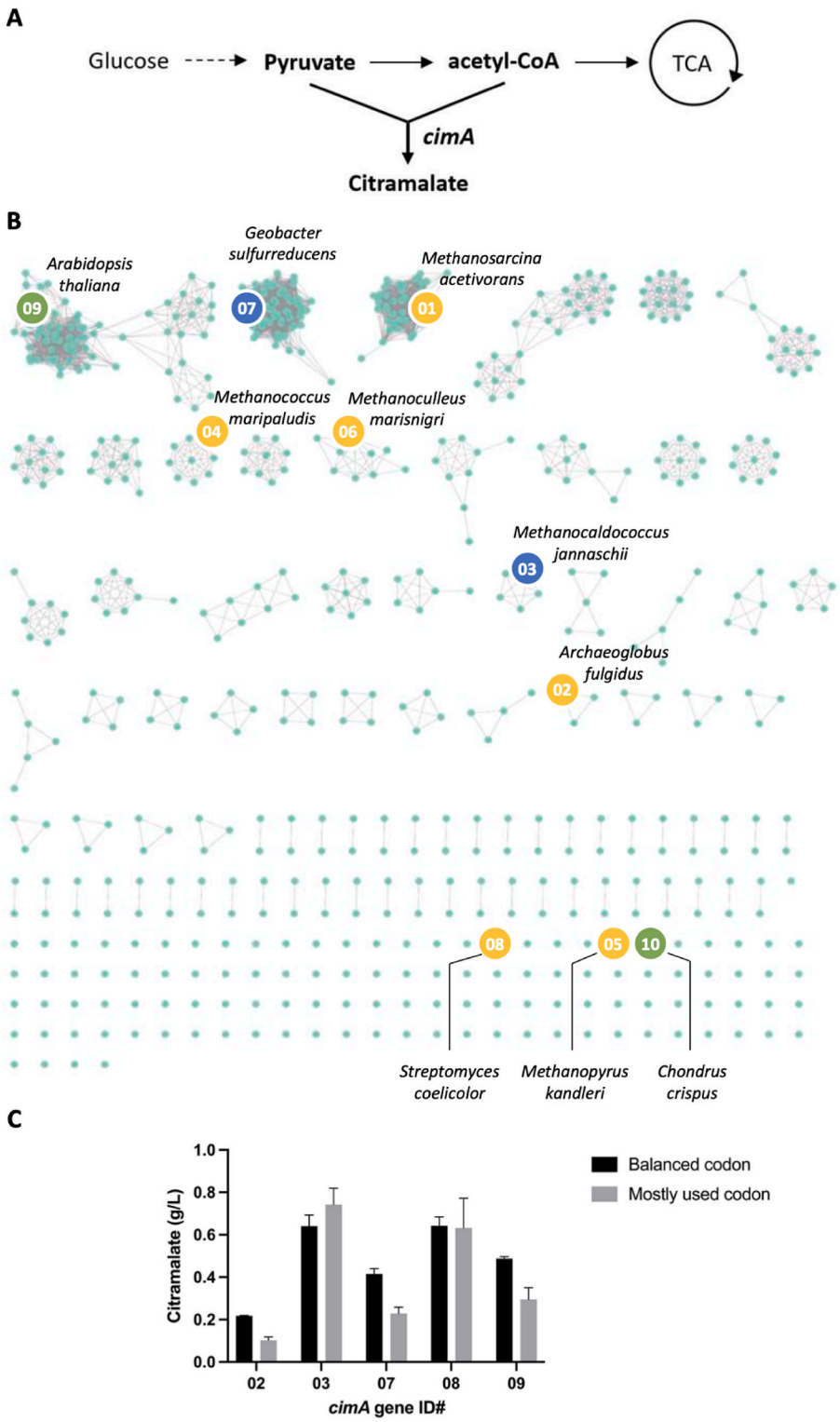

Fig. 2. Identification of a more active *cimA* variant for citramalate production in *I. orientalis* SD108. (A) Schematic representation of the pathway for citramalate production. Citramalate is formed from condensation between pyruvate and acetyl-CoA. (B) The SSN analysis was used for target gene selection. The *cimA* variants that have been previously characterized are denoted with blue circles. The *cimA* variants of eukaryotic origin are denoted with green circles. The orange circles indicate the *cimA* variants randomly selected from different clades. The number in each dot represents the synthetic *cimA* gene ID. The sequences of those genes are listed in Supplementary Tables S3 and S4. (C) Citramalate production from *I. orientalis* SD108 expressing five active genes in a plasmid with two different codon optimization strategies using BOOST (Oberortner et al., 2017). The black bars indicate genes optimized with "balanced" codon usage. The gray bars represent genes optimized with "mostly used" codon usage. These samples were measured at 48 h after cultivation. All experiments were done in technical triplicate. (For interpretation of the references to color in this figure legend, the reader is referred to the Web version of this article.)

high-performing CimA variants for their activities to produce citramalate through an *in vitro* analysis using pyruvate and acetyl-CoA as substrates. We collected the data in technical triplicate. The calculated specific activities for *Methanocaldococcus jannasch* CimA and *Streptomyces coelicolor* CimA are 0.38 (SD = 0.023) and 0.55 (SD = 0.2) μmol/min/mg, respectively. The strains carrying the other three *cimA* genes showed much lower citramalate production, 0.1–0.4 g/L. Thus, we identified two *cimA* variants that have good activity. Because gene #03 ("mostly used") produced slightly more citramalate than the others, we selected it for subsequent studies. However, the other variants could also be integrated into *I. orientalis* to effectively increase the copy number of *cimA*, relieving the concern of potential recombination among the repeats if the identical sequence were integrated for multiple times.

3.3. Transposon-mediated genome integration for citramalate production

We selected the piggyBac transposon system to integrate the *cimA* gene into the *I. orientalis* genome. This system can integrate multiple

copies of a payload into random locations (any TTAA sites) of the genome. In this way, we could simultaneously evaluate the effects of different integration locations and copy numbers of the *cimA* gene on citramalate production. A plasmid, pWS-URA-hPB7-GFP-CimA-LEU containing a hyperactive piggyBac transposase gene (hPB7) and the transposon, GFP-CimA-LEU gene cassette, flanked by inverted repeat sequences (IRSs) was constructed. This integration cassette is also flanked by extra TTAA, so we could expect the cassette to be integrated into any TTAA sites in the *I. orientalis* genome (Fig. 3A). After transformation of pWS-URA-hPB7-GFP-CimA-LEU, we randomly picked 50 colonies from the SC-LEU plate and determined whether the *cimA* transposon integration cassette was integrated using flow cytometry. All 50 strains stably expressed GFP, suggesting the successful integration of the cassette into the genome (Supplementary Fig. S3). These strains were cultured in SC-LEU media containing 50 g/L glucose for 5 days, and citramalate production was measured. The lowest and highest citramalate production differed 6-fold, ranging from 0.4 to 2.5 g/L (Fig. 3B). We subsequently selected the top four producers and counter-selected to cure the plasmids and to ensure stable *cimA* expression. For simplicity, these four strains, #12, #20, #33, and #40, were renamed SB814, SB815, SB816, and SB817, respectively.

To determine the integration locations and copy number of *cimA*, we performed PacBio sequencing and summarized the results in Table 1 and Supplementary Table S5. We identified the copy number of *cimA* and the integration sites by aligning raw reads to the genome sequence of *I. orientalis* SD108 v2.0 from the JGI MycoCosm, The Fungal Genome Resource database (Grigoriev et al., 2014). We also identified the neighborhood genes of each *cimA* integration site based on the data retrieved from the JGI IMG Integrated Microbial Genomes and Microbiomes database (Chen et al., 2019). The strain SB814 had the most *cimA* copies in the genome (six). Two of the six copies disrupted a hypothetical protein gene (these two loci are allelic to each other). Strains SB815, SB816, and SB817 each had two *cimA* copies. The *cimA* in SB815 did not integrate into any known gene, while the *cimA* integration site of SB816 disrupted a myosin protein heavy chain (MHC) gene. The *cimA* in SB817 destroyed a AAA family ATPase gene and its allele, and its transposase recognition was CTAA, not TTAA. These four genome-integrated-*cimA* strains were cultured, and their ability to produce citramalate was further evaluated.

3.4. Production of citramalate from cimA-integrated I. orientalis strains

To compare the performance of different strains, we cultured the *I. orientalis* SD108 *ΔURA3* strain, that same strain but harboring the *cimA* plasmid (pCimA03), and the top four citramalate producers (SB814, SB815, SB816, and SB817) with the genome-integrated-*cimA* in both SC and YPD media containing 50 g/L glucose for 3 days. In the SC medium, glucose consumption and growth rate were reduced for all engineered strains (Fig. 4). They did all produce citramalate but in different amounts. The four genome-integrated strains all produced significantly more citramalate than their plasmid-based counterpart did (Fig. 4A and 5A). In particular, SB814 and SB816 produced the most citramalate, with a titer of 2.0 g/L and a yield of up to 7% mol citramalate/mol consumed glucose (Fig. 4A). In contrast, all strains cultured in the YPD medium consumed 50 g/L glucose within 24 h (Fig. 5B). Interestingly, cultures in the YPD medium did not increase citramalate production as much as cultures in the SC medium did, but the YPD medium doubled biomass and ethanol production (Fig. 5C and F). Supplementary Fig. S4 shows the pH values of the YPD medium containing SB814 over 96 h. The results support the viability of using *I. orientalis* as a host platform for producing citramalate under low-pH fermentation conditions, as the pH was observed to rapidly drop to 3.2 within 24 h and remain stable

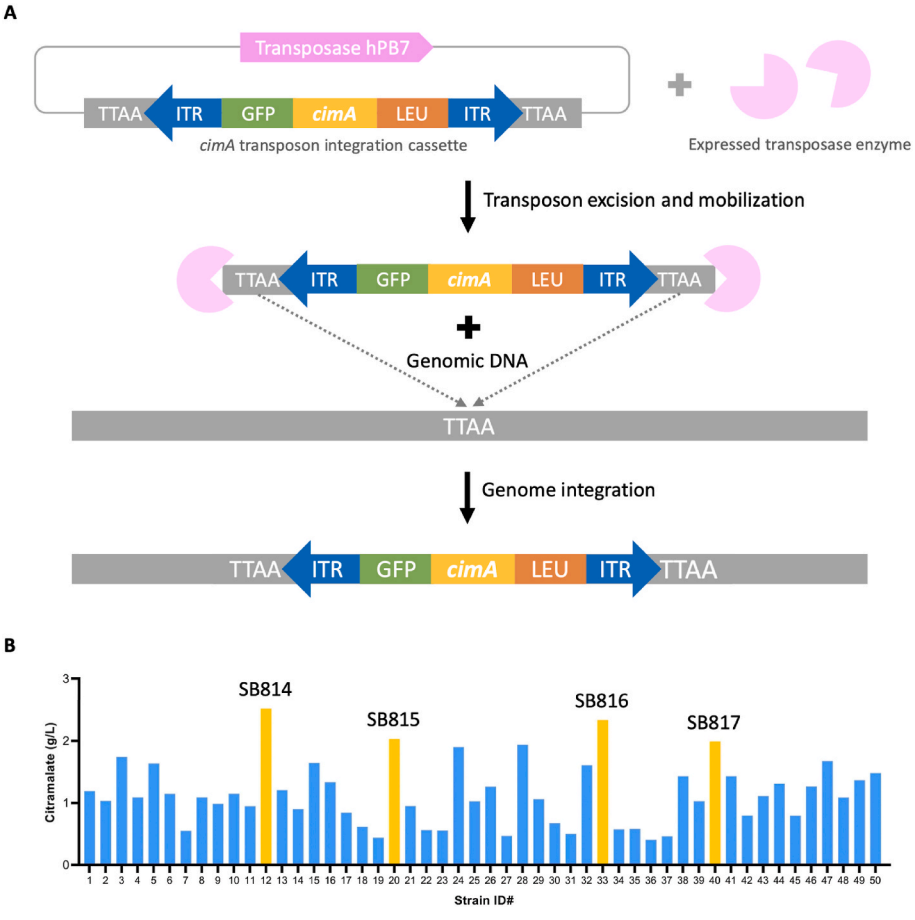

Fig. 3. Random integration of *cimA* into *I. orientalis* and citramalate production. (A) The schematics showing the PiggyBac transposon-mediated genome integration of *cimA*. The plasmid containing the *cimA* transposon integration cassette (ITR-GFP-CimA-LEU-ITR) and PiggyBac transposase gene (hpB7) was transformed into *I. orientalis* SD108. Catalyzed by the PiggyBac transposase, this integration cassette was randomly integrated into the 'TTAA' sites in the *I. orientalis* genome. This system can also integrate multiple copies of the integration cassette. (B) Comparison of citramalate production from the *cimA* integration variants. The four best producers, SB814 (Strain ID#12), SB815 (Strain ID#20), SB816 (Strain ID#33), and SB817 (Strain ID#40) are highlighted in yellow. The experiments were carried out with single replicate. Citramalate production levels at 120 h were compared. (For interpretation of the references to color in this figure legend, the reader is referred to the Web version of this article.)

Table 1
Copy number and integration sites of *cimA*-integrated *I. orientalis* strains.

I. orientalis strain	Copy number	Transposase recognition	Integration site/allele site[a]	Gene that has been disrupted[b]
SB814	6	TTAA	Issorie2|scaffold_1:422225-42228/scaffold_13:305227-305230	None
		TTAA	Issorie2|scaffold_29:112489-112492/scaffold_31:102246-102249	Hypothetical protein
		TTAA	Issorie2|scaffold_10: 140124-140138/scaffold_1:1572178–1572193	None
SB815	2	TTAA	Issorie2|scaffold_1: 2431243–2431246/scaffold_20:160384-160387	None
SB816	2	TTAA	Issorie2|scaffold_2:718184-718187	None
		TTAA	Issorie2|scaffold_34:30875-30987	Myosin protein heavy chain
SB817	2	CTAA	Issorie2|scaffold_53:4781–4784/scaffold_1:72387-72390	AAA family ATPase

[a] The integration sites were identified based on the JGI MycoCosm, The Fungal Genome Resource.
[b] The gene neighborhood data was retrieved from the JGI IMG Integrated Microbial Genome & Microbiomes database.

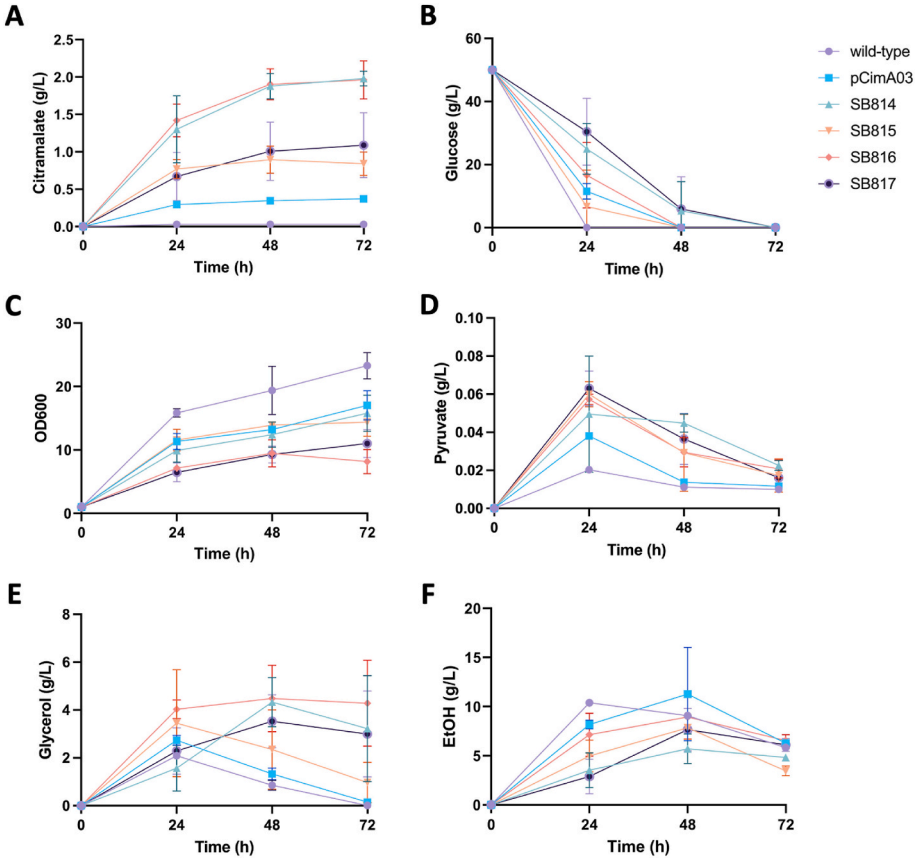

Fig. 4. Citramalate production from the *cimA*-integrated *I. orientalis* strains in SC medium. Strains were cultivated in SC containing 50 g/L glucose at 30 °C at 250 rpm for 72 h. (A) citramalate production, (B) glucose consumption, and (C) growth. Byproducts shown are (D) pyruvate, (E) glycerol, and (F) EtOH, measured using LC-MS. All experiments were performed in biological triplicate.

between 3.2 and 3.4 until the end of the cultivation period.

4. Discussion

4.1. Identification of optimal CimA variants for citramalate production in I. orientalis

Since citramalate synthase (CimA, EC 2.3.1.182) was identified from a thermophilic methanogenic archaea, *M. jannaschii* (Howell et al., 1999), only a few CimA variants have been evaluated in an *E. coli* heterologous expression system for citramalate biosynthesis (Webb et al., 2018; Wu and Eiteman, 2016). With the rapid increase in the abundance of protein sequences in public databases, we sought to identify more efficient CimA from nature. We therefore built a CimA SSN to investigate this possibility and guide target gene selection. In our SSN (Fig. 2B), sequences sharing over 80% identities were grouped into the same cluster. By selecting candidate genes from different clusters, we were able to avoid synthesizing genes with high similarities. In this way, we identified five *cimA* genes that are active in *I. orientalis*. Their origins are *Archaeoglobus fulgidus* (gene #02), *M. jannaschii* (gene #03), *Geobacter sulfurreducens* (gene #07), *S. coelicolor* (gene #08), and *Arabidopsis thaliana* (gene #09). Among them, the *cimA* genes from *M. jannaschii* and *G. sulfurreducens* were previously functionally expressed in *E. coli.* Whereas the other three were verified in *I. orientalis* for the first time. We did not identify CimA variants that resulted in higher citramalate yields than that from *M. jannaschii*. Although it has only 31.2% sequence identity to CimA from *M. jannaschii,* CimA from *S. coelicolor* enabled to the production of a similar level of citramalate (Fig. 2C). Supplementary Table S6 shows the sequence identity among different CimA genes. These CimA variants generally show only 30–50% identities at the protein level. This result shows that the sequence diversity of CimA is high; no obvious trend for sequence-function relationships was found.

Another factor that impacts citramalate production is the level of functional CimA expression. Codon optimization is a common strategy

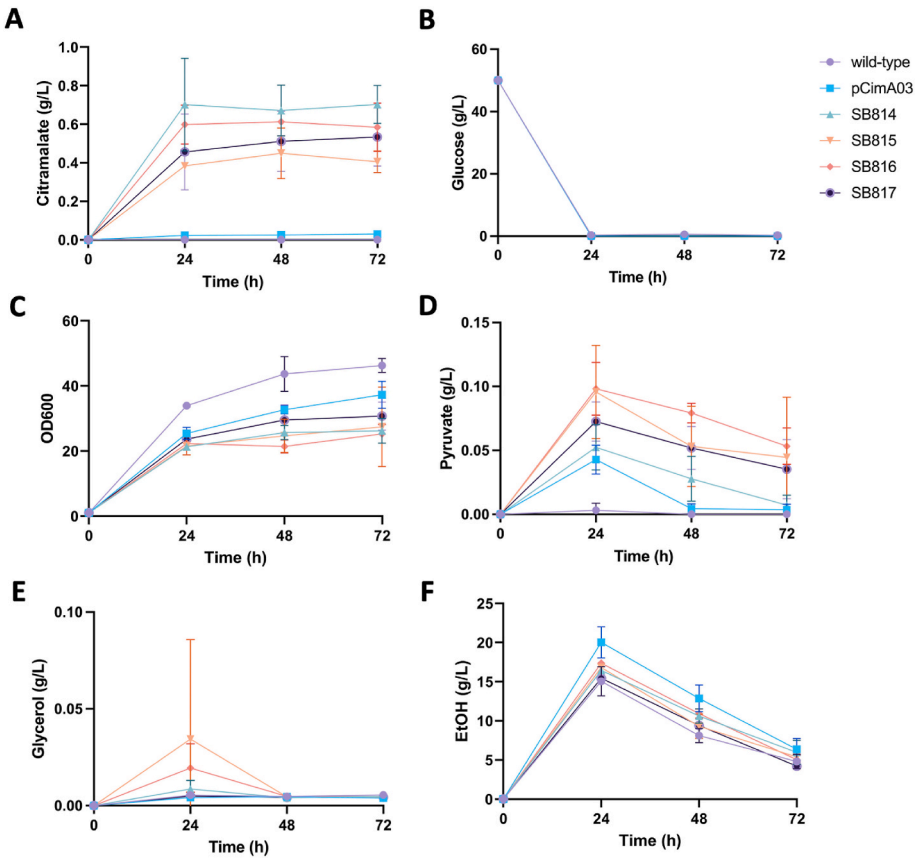

Fig. 5. Citramalate production from the *cimA*-integrated *I. orientalis* strains in YPD medium. Strains were cultivated in YPD containing 50 g/L glucose at 30 °C at 250 rpm for 72 h. (A) citramalate production, (B) glucose consumption, and (C) growth. Byproducts shown are (D) pyruvate, (E) glycerol, and (F) EtOH, measured using LC-MS. All experiments were performed in biological triplicate.

to increase the expression level of proteins (Plotkin and Kudla, 2011). We therefore used two different codon optimization parameters offered by the JGI BOOST; one is "balanced" and the other is "mostly used." In "balanced" codon optimization, BOOST selects the most-used and second-most-used codon for each amino acid as evenly used as possible during the process (Oberortner et al., 2017). This mitigates the sequence complexity that may arise by using only the most-preferred codon, as is done when using the "mostly used" optimization strategy. Since low-complexity DNA reduces the occurrence of repeats, secondary structure, and sequence stretches with extreme GC content, we expected DNA to be readily manufactured, and could potentially avoid mRNA secondary structure that might affect protein expression. Although we did not evaluate the CimA protein level in this study, the "balanced" codon-optimized *cimA* genes generally produced more citramalate (Fig. 3C). This difference between "balanced" and "mostly used" in the plasmid expression system is subtle. Access to multiple *cimA* variations is helpful because eventually, numerous copies of *cimA* genes need to be integrated into the genome to enhance the production level of citramalate, and the potential instability factor such as recombination among identical sequences needs to be mitigated.

4.2. *cimA* genome integration by piggyBac transposase system

Plasmid expression systems are typically unstable and not favorable for metabolic engineering. In contrast, genome integration is a better approach to stably maintain heterologous genes. The gene numbers and integration locations are also known to be crucial for heterologous gene expression (Da Silva and Srikrishnan, 2012; Flagfeldt et al., 2009). Our top producer, SB814, has the most (six) *cimA* copies in the genome. Compared with the other three strains, which have only two copies (SB815, SB816, and SB817), SB814 had the highest citramalate production in both SC and YPD medium (Figs. 4A and 5A). However, one of the strains with only two *cimA* copies, SB816, had a production level similar to that of SB814 in the SC medium (Fig. 4A), and had only a slightly lower production level than SB814 in the YPD medium (Fig. 5A). This may be because the integration site in SB816 allows a high-level gene expression or expression dynamics more suitable for citramalate production. Although the difference in gene expression level requires further verification, the result suggests the potential of these integration loci providing more choices for future strain engineering. In general, we only recommend using GFP expression and flow cytometry to facilitate the screening of integrants rather than as a guide to report the production of a target compound. This is because a high titer is a result from collective factors such as enzyme concentration and activity, substrate availability, depletion of important central metabolites, toxicity of intermediates and products, and key enzyme expression dynamics. In our previous study with optimization of shikimate production in a different yeast host, the correlation between GFP expression and high production was also not observed (Zhao et al., 2020).

Considering random integration could accidentally disrupt coding regions, the fatality of the disruption needs to be examined. In our case, although the integration sites in three *cimA*-integrated *I. orientalis* strains disrupted genes (Table 1), including a hypothetical protein gene in SB814, a myosin protein heavy chain (MHC) gene in SB816, and an AAA family ATPase gene in SB817, the strains' growth showed that no fatal effects had occurred. Their growth rates were also not dramatically different than that of SB815, which did not have any genes disrupted (Figs. 4C and 5C). The MHC gene was labeled non-essential for cell survival under laboratory growth conditions in *S. cerevisiae* (Rodriguez and Paterson, 1990). The AAA family ATPase contains many genes with

similar functions. According to the annotation data of Pfam (PF00004) in the JGI's MycoCosm database, *I. orientalis* has 32 AAA family ATPases (Grigoriev et al., 2014). The disrupted gene in SB817 was likely compensated by other ATPases, so no fatal effect occurred. Although the growth rates of all four *cimA*-integrated *I. orientalis* strains were slower than that of the wild-type and the strain expressing *cimA* in a plasmid, those four strains still reached the late logarithmic phase at 24 h. The slower growth might also have been caused by the extra expenditure for producing a foreign product or LEU2 auxotroph.

Recently, a study describes a Hermes transposon-mediated random integration method in *Scheffersomyces stipitis* by transforming a non-replicable circular DNA allows the skip of the plasmid curing step and efficiently removes false positive clones (Zhao et al., 2020). We transformed a nonreplicable circular DNA containing the ITR flanked GFP-CimA-LEU fragment and PiggyBac cassette but were only able to get very few colonies on the plate. The number of colonies was too few for effective library construction and screening. Previous studies have shown that Nonhomologous-End-Joining (NHEJ) is involved in the double-stranded DNA break repair in transposition (Yant and Kay, 2003; Yu et al., 2004). However, *I. orientalis* is a homologous recombination-dominant strain (Cao et al., 2020), and the transient expression of PiggyBac in the nonreplicable carrier may not be sufficient for transposition. Future studies to identify important NHEJ-related proteins and overexpress these proteins may help streamline the protocol via a nonreplicable circular DNA in *I. orientalis*.

4.3. Citramalate production from cimA-integrated I. orientalis strains and future optimization

The much higher production yielded by the *cimA*-integrated strains in general than the one expressing *cimA* in a plasmid and distinctly different levels of citramalate production among the four integration strains (Figs. 4A and 5A) support the validity of using the piggyBac transposase system to integrate the heterologous gene directly into the *I. orientalis* genome and exploring the impacts of integration loci and copy numbers on citramalate production.

In general, we observed higher citramalate production from cultures using the SC medium (Fig. 4A) than from those using the YPD medium (Fig. 5A). In the YPD medium, cells quickly consumed glucose and mainly diverted the carbon to their growth and to ethanol production (Fig. 5C and F). In both medium conditions, post glucose depletion, the strains shifted their metabolism to consume ethanol for growth (Figs. 4F and 5F). However, ethanol consumption did not lead to further citramalate production.

Deletion of pyruvate decarboxylase (*PDC*) and/or downregulation of the TCA cycle have been shown to reduce efflux to ethanol synthesis (Webb et al., 2018; Wu and Eiteman, 2016; Xiao et al., 2014). However, it is known that the deletion of *PDC* will negatively affect the cytosolic synthesis of acetyl-CoA. To increase cytosolic acetyl-CoA level, expression of pyruvate dehydrogenase (Nielsen, 2014), and/or non-oxidative glycolysis (NOG) pathways (Meadows et al., 2016) may be considered. Alternatively, it is also conceivable to express CimA in the mitochondria, where both pyruvate and acetyl-CoA are accessible through pyruvate dehydrogenase activity.

The engineered strains, in particular the *cimA*-integrated strains, accumulated glycerol more than the wild-type strain in the SC medium (Fig. 4E), suggesting that the expression of citramalate synthase may also cause metabolic imbalance (Vemuri et al., 2007). Conversion of glucose into citramalate yields excess reducing co-factors, which might be offset by the production of glycerol. Production of acetyl-CoA through pyruvate oxidase and the NOG pathway may also mitigate the redox imbalance caused by citramalate production and help increase citramalate yield. Combining the above strategies to further increase the yield of citramalate should be considered for future strain engineering.

5. Conclusion

Bio-based organic acids are important chemical building blocks for the production of commodity chemicals and materials with diverse applications. The non-conventional chassis *I. orientalis* has an extraordinary ability to tolerate diverse industrially relevant stresses (e.g., low pH and inhibitors in lignocellulosic biomass hydrolysates), and it as a chassis for the production of organic acids could potentially reduce the cost and environmental footprint of organic acid production by 30% compared with using conventional species as chassis. For non-model strains, genetic engineering tools are limited, and the Design-Build-Test-Learn cycle tends to be slow. Therefore, we decided to use the piggyBac transposon system to identify optimal integration loci and copy numbers for citramalate production. We used the *M. jannaschii cimA*, which performed the best in *I. orientalis* according to our initial screening. Four strains, SB814 through SB817, showed high citramalate production after random integration of this *cimA* gene using the piggyBac system. Further characterization indicated that these strains contain 2 to 6 copies of the *cimA* gene in their genomes, and their integration sites were diverse. We demonstrated that SB814 and SB816 produced the highest amount of citramalate, 2 g/L, which was 6-fold higher than that of their plasmid counterpart. These results demonstrated the efficacy of the piggyBac transposon system for rapid exploration of integration sites and copy numbers of important metabolic genes, which allowed us to create high-production strains.

CRediT authorship contribution statement

Zong-Yen Wu: Investigation, Visualization, Writing – original draft. **Wan Sun:** Investigation, Validation, Writing – original draft. **Yihui Shen:** Investigation, Validation, Writing – original draft. **Jimmy Pratas:** Investigation. **Patrick F. Suthers:** Investigation. **Ping-Hung Hsieh:** Investigation. **Sudharsan Dwaraknath:** Investigation. **Joshua D. Rabinowitz:** Supervision. **Costas D. Maranas:** Supervision. **Zengyi Shao:** Conceptualization, Supervision, Writing – review & editing. **Yasuo Yoshikuni:** Conceptualization, Supervision, Writing – review & editing.

Declaration of competing interest

The authors declare that they have no known competing financial interests or personal relationships that could have appeared to influence the work reported in this paper.

Data availability

Data will be made available on request.

Acknowledgements

This work was funded by the DOE Center for Advanced Bioenergy and Bioproducts Innovation (U.S. Department of Energy, Office of Science, Office of Biological and Environmental Research under Award Number DE-SC0018420 and DE-AC02-05CH11231). The work conducted by the U.S. Department of Energy Joint Genome Institute (https://ror.org/04xm1d337), a DOE Office of Science User Facility, is supported by the Office of Science of the U.S. Department of Energy operated under Contract No. DE-AC02-05CH11231. Any opinions, findings, and conclusions or recommendations expressed in this publication are those of the author(s) and do not necessarily reflect the views of the U.S. Department of Energy. We thank Anita Wahler for professional editing.

Appendix A. Supplementary data

Supplementary data to this article can be found online at https://doi.

org/10.1016/j.mec.2023.e00220.

References

Bhagwat, S.S., Li, Y., Cortés-Peña, Y.R., Brace, E.C., Martin, T.A., Zhao, H., Guest, J.S., 2021. Sustainable production of acrylic acid via 3-hydroxypropionic acid from lignocellulosic biomass. ACS Sustainable Chem. Eng. 9, 16659–16669.

Bindel, M., 2016. 3-hydroxypropionic Acid Production by Recombinant Yeasts. US Patent, 9365875.

Cao, M., Fatma, Z., Song, X., Hsieh, P.-H., Tran, V.G., Lyon, W.L., Sayadi, M., Shao, Z., Yoshikuni, Y., Zhao, H., 2020. A genetic toolbox for metabolic engineering of Issatchenkia orientalis. Metab. Eng. 59, 87–97.

Chambers, M.C., Maclean, B., Burke, R., Amodei, D., Ruderman, D.L., Neumann, S., Gatto, L., Fischer, B., Pratt, B., Egertson, J., Hoff, K., Kessner, D., Tasman, N., Shulman, N., Frewen, B., Baker, T.A., Brusniak, M.-Y., Paulse, C., Creasy, D., Flashner, L., Kani, K., Moulding, C., Seymour, S.L., Nuwaysir, L.M., Lefebvre, B., Kuhlmann, F., Roark, J., Rainer, P., Detlev, S., Hemenway, T., Huhmer, A., Langridge, J., Connolly, B., Chadick, T., Holly, K., Eckels, J., Deutsch, E.W., Moritz, R.L., Katz, J.E., Agus, D.B., MacCoss, M., Tabb, D.L., Mallick, P., 2012. A cross-platform toolkit for mass spectrometry and proteomics. Nat. Biotechnol. 30, 918–920.

Chen, I.-M.A., Chu, K., Palaniappan, K., Pillay, M., Ratner, A., Huang, J., Huntemann, M., Varghese, N., White, J.R., Seshadri, R., Smirnova, T., Kirton, E., Jungbluth, S.P., Woyke, T., Eloe-Fadrosh, E.A., Ivanova, N.N., Kyrpides, N.C., 2019. IMG/M v.5.0: an integrated data management and comparative analysis system for microbial genomes and microbiomes. Nucleic Acids Res. 47, D666–D677.

Curson, A.R.J., Burns, O.J., Voget, S., Daniel, R., Todd, J.D., McInnis, K., Wexler, M., Johnston, A.W.B., 2014. Screening of metagenomic and genomic libraries reveals three classes of bacterial enzymes that overcome the toxicity of acrylate. PLoS One 9, e97660.

Da Silva, N.A., Srikrishnan, S., 2012. Introduction and expression of genes for metabolic engineering applications in Saccharomyces cerevisiae. FEMS Yeast Res. 12, 197–214.

Dixit, M., Mathur, V., Gupta, S., Baboo, M., Sharma, K., Saxena, N.S., Others, 2009. Investigation of miscibility and mechanical properties of PMMA/PVC blends. J. Optoelectron. Adv. Mater. Rapid Commun 3, 1099–1105.

Flagfeldt, D.B., Siewers, V., Huang, L., Nielsen, J., 2009. Characterization of chromosomal integration sites for heterologous gene expression in Saccharomyces cerevisiae. Yeast 26, 545–551.

Frazer, R.Q., Byron, R.T., Osborne, P.B., West, K.P., 2005. PMMA: an essential material in medicine and dentistry. J. Long Term Eff. Med. Implants 15, 629–639.

Gerlt, J.A., Bouvier, J.T., Davidson, D.B., Imker, H.J., Sadkhin, B., Slater, D.R., Whalen, K.L., 2015. Enzyme Function Initiative-Enzyme Similarity Tool (EFI-EST): a web tool for generating protein sequence similarity networks. Biochim. Biophys. Acta 1854, 1019–1037.

Grand View Research, 2019. PMMA market size worth $8.16 billion by 2025 | CAGR: 8.4% [WWW Document]. URL. https://www.grandviewresearch.com/press-release/global-polymethyl-methacrylate-pmma-industry (accessed 12.19.21).

Grigoriev, I.V., Nikitin, R., Haridas, S., Kuo, A., Ohm, R., Otillar, R., Riley, R., Salamov, A., Zhao, X., Korzeniewski, F., Smirnova, T., Nordberg, H., Dubchak, I., Shabalov, I., 2014. MycoCosm portal: gearing up for 1000 fungal genomes. Nucleic Acids Res. 42, D699–D704.

Howell, D.M., Xu, H., White, R.H., 1999. (R)-citramalate synthase in methanogenic archaea. J. Bacteriol. 181, 331–333.

Johnson, D.W., Eastham, G.R., Poliakoff, M., Huddle, T.A., 2015. Method of Producing Arcylic and Methacrylic Acid. US Patent, 8933179.

Lebeau, J., Efromson, J.P., Lynch, M.D., 2020. A review of the biotechnological production of methacrylic acid. Front. Bioeng. Biotechnol. 8, 207.

Li, X., Burnight, E.R., Cooney, A.L., Malani, N., Brady, T., Sander, J.D., Staber, J., Wheelan, S.J., Joung, J.K., McCray Jr., P.B., Bushman, F.D., Sinn, P.L., Craig, N.L., 2013. piggyBac transposase tools for genome engineering. Proc. Natl. Acad. Sci. U.S. A. 110, E2279–E2287.

Mahboub, M.J.D., Dubois, J.-L., Cavani, F., Rostamizadeh, M., Patience, G.S., 2018. Catalysis for the synthesis of methacrylic acid and methyl methacrylate. Chem. Soc. Rev. 47, 7703–7738.

Meadows, A.L., Hawkins, K.M., Tsegaye, Y., Antipov, E., 2016. Rewriting yeast central carbon metabolism for industrial isoprenoid production. Nature 537, 694–697.

Nagai, K., Ui, T., 2004. Trends and future of monomer-MMA technologies. Sumitomo Chem 2, 4–13.

Nakamura, yasukazu, 2007. Codon Usage Database [WWW Document]. Codon Usage Database. URL https://www.kazusa.or.jp/codon/.

Nielsen, J., 2014. Synthetic biology for engineering acetyl coenzyme A metabolism in yeast. mBio 5, e02153.

Oberortner, E., Cheng, J.-F., Hillson, N.J., Deutsch, S., 2017. Streamlining the design-to-build transition with build-optimization software tools. ACS Synth. Biol. 6, 485–496.

Park, H.J., Bae, J.-H., Ko, H.-J., Lee, S.-H., Sung, B.H., Han, J.-I., Sohn, J.-H., 2018. Low-pH production of d-lactic acid using newly isolated acid tolerant yeast Pichia kudriavzevii NG7. Biotechnol. Bioeng. 115, 2232–2242.

Plotkin, J.B., Kudla, G., 2011. Synonymous but not the same: the causes and consequences of codon bias. Nat. Rev. Genet. 12, 32–42.

Risso, C., Van Dien, S.J., Orloff, A., Lovley, D.R., Coppi, M.V., 2008. Elucidation of an alternate isoleucine biosynthesis pathway in Geobacter sulfurreducens. J. Bacteriol. 190, 2266–2274.

Rodriguez, J.R., Paterson, B.M., 1990. Yeast myosin heavy chain mutant: maintenance of the cell type specific budding pattern and the normal deposition of chitin and cell wall components requires an intact myosin heavy chain gene. Cell Motil Cytoskeleton 17, 301–308.

Shannon, P., Markiel, A., Ozier, O., Baliga, N.S., Wang, J.T., Ramage, D., Amin, N., Schwikowski, B., Ideker, T., 2003. Cytoscape: a software environment for integrated models of biomolecular interaction networks. Genome Res. 13, 2498–2504.

Shao, Z., Zhao, H., 2014. Manipulating natural product biosynthetic pathways via DNA assembler. Curr. Protoc. Chem. Biol. 6, 65–100.

Shao, Z., Luo, Y., Zhao, H., 2012. DNA assembler method for construction of zeaxanthin-producing strains of Saccharomyces cerevisiae. Methods Mol. Biol. 898, 251–262.

Sugimoto, N., Engelgau, P., Jones, A.D., Song, J., Beaudry, R., 2021. Citramalate synthase yields a biosynthetic pathway for isoleucine and straight- and branched-chain ester formation in ripening apple fruit. Proc. Natl. Acad. Sci. U.S.A. 118 https://doi.org/10.1073/pnas.2009988118.

Sun, W., Vila-Santa, A., Liu, N., Prozorov, T., Xie, D., Faria, N.T., Ferreira, F.C., Mira, N. P., Shao, Z., 2020. Metabolic engineering of an acid-tolerant yeast strain Pichia kudriavzevii for itaconic acid production. Metab Eng Commun 10, e00124.

Suthers, P.F., Dinh, H.V., Fatma, Z., Shen, Y., Chan, S.H.J., Rabinowitz, J.D., Zhao, H., Maranas, C.D., 2020. Genome-scale metabolic reconstruction of the non-model yeast Issatchenkia orientalis SD108 and its application to organic acids production. Metab Eng Commun 11, e00148.

Toivari, M., Vehkomäki, M.-L., Nygård, Y., Penttilä, M., Ruohonen, L., Wiebe, M.G., 2013. Low pH D-xylonate production with Pichia kudriavzevii. Bioresour. Technol. 133, 555–562.

Tran, V.G., Cao, M., Fatma, Z., Song, X., Zhao, H., 2019. Development of a CRISPR/Cas9-Based tool for gene deletion in Issatchenkia orientalis. mSphere 4. https://doi.org/10.1128/mSphere.00345-19.

Vemuri, G.N., Eiteman, M.A., McEwen, J.E., Olsson, L., Nielsen, J., 2007. Increasing NADH oxidation reduces overflow metabolism in Saccharomyces cerevisiae. Proc. Natl. Acad. Sci. U.S.A. 104, 2402–2407.

Wagner, J.M., Williams, E.V., Alper, H.S., 2018. Developing a piggyBac transposon system and compatible selection markers for insertional mutagenesis and genome engineering in Yarrowia lipolytica. Biotechnol. J. 13, e1800022.

Webb, J.P., Arnold, S.A., Baxter, S., Hall, S.J., Eastham, G., Stephens, G., 2018. Efficient bio-production of citramalate using an engineered Escherichia coli strain. Microbiology 164, 133–141.

Wu, X., Eiteman, M.A., 2016. Production of citramalate by metabolically engineered Escherichia coli. Biotechnol. Bioeng. 113, 2670–2675.

Xiao, H., Shao, Z., Jiang, Y., Dole, S., Zhao, H., 2014. Exploiting Issatchenkia orientalis SD108 for succinic acid production. Microb. Cell Factories 13, 121.

Xiao, Han, Shao, Zengyi, Jiang, Yu, Dole, Sudhanshu, Zhao, Huimin, 2014. "Exploiting Issatchenkia orientalis SD108 for succinic acid production. Microb. Cell Factories 13 (August), 121.

Yant, S.R., Kay, M.A., 2003. Nonhomologous-end-joining factors regulate DNA repair fidelity during Sleeping Beauty element transposition in mammalian cells. Mol. Cell Biol. 23, 8505–8518.

Yu, J., Marshall, K., Yamaguchi, M., Haber, J.E., Weil, C.F., 2004. Microhomology-dependent end joining and repair of transposon-induced DNA hairpins by host factors in Saccharomyces cerevisiae. Mol. Cell Biol. 24, 1351–1364.

Yusa, K., Zhou, L., Li, M.A., Bradley, A., Craig, N.L., 2011. A hyperactive piggyBac transposase for mammalian applications. Proc. Natl. Acad. Sci. U.S.A. 108, 1531–1536.

Zafar, M.S., 2020. Prosthodontic applications of polymethyl methacrylate (PMMA): an update. Polymers 12. https://doi.org/10.3390/polym12102299.

Zhao, Y., Yao, Z., Ploessl, D., Ghosh, S., Monti, M., Schindler, D., Gao, M., Cai, Y., Qiao, M., Yang, C., Cao, M., Shao, Z., 2020. Leveraging the Hermes transposon to accelerate the development of nonconventional yeast-based microbial cell factories. ACS Synth. Biol. 9, 1736–1752.

Zhao, Yuxin, Yao, Zhanyi, Ploessl, Deon, Ghosh, Saptarshi, Monti, Marco, Schindler, Daniel, Gao, Meirong, et al., 2020. "Leveraging the Hermes transposon to accelerate the development of nonconventional yeast-based microbial cell factories. ACS Synth. Biol. 9 (7), 1736–1752.